Title:

Analysis of physical pore space characteristics of two pyrolytic biochars and potential as microhabitat

Authors:

Laura S. Schnee
University of Bremen, Soil Microbial Ecology
Germany
laura.schnee@yahoo.de

Stefan Knauth
University of Bremen, Soil Microbial Ecology
Germany
sknauth@uni-bremen.de

Simona Hapca
Abertay University Dundee, SIMBIOS Centre
UK
s.hapca@abertay.ac.uk

Present address: University of Dundee, School of Medicine, Dundee Epidemiology and Biostatistics Unit (DEBU)
s.z.hapca@dundee.ac.uk

Wilfred Otten
Abertay University Dundee, SIMBIOS Centre
UK
w.otten@abertay.ac.uk

Present address:

School of Water Energy and Environment, Cranfield University, Cranfield, UK

Thilo Eickhorst
University of Bremen, Soil Microbial Ecology
Germany
eickhorst@uni-bremen.de

Corresponding author:

Thilo Eickhorst
University of Bremen, Soil Microbial Ecology
Leobener Str., UFT
28359 Bremen
Germany
eickhorst@uni-bremen.de

Analysis of physical pore space characteristics of two pyrolytic biochars and potential as microhabitat

Laura S. Schnee, Stefan Knauth, Simona Hapca, Wilfred Otten, Thilo Eickhorst*

*) eickhorst@uni-bremen.de

Keywords

Biochar, microbial colonisation, pore geometry, habitat quality

Abstract

Background and Aims

Biochar amendment to soil is a promising practice of enhancing productivity of agricultural systems. The positive effects on crops are often attributed to a promotion of beneficial soil microorganisms while suppressing pathogens. This study aims to determine the influence of biochar feedstock on (i) spontaneous and fungi inoculated microbial colonisation of biochar particles and (ii) physical pore space characteristics of native and fungi colonised biochar particles which impact microbial habitat quality.

Methods

Pyrolytic biochars from mixed woods and *Miscanthus* were investigated towards spontaneous colonisation by classical microbiological isolation, phylogenetic identification of bacterial and fungal strains, and microbial respiration analysis. Physical pore space characteristics of biochar particles were determined by X-ray µ-CT. Subsequent 3D image analysis included porosity, surface area, connectivities, and pore size distribution.

Results

Microorganisms isolated from Wood biochar were more abundant and proliferated faster than those from the *Miscanthus* biochar. All isolated bacteria belonged to gram-positive bacteria and were feedstock specific. Respiration analysis revealed higher microbial activity for Wood biochar after water and substrate amendment while basal respiration was on the same low level for both biochars.

Differences in porosity and physical surface area were detected only in interaction with biochar-specific colonisation. *Miscanthus* biochar was shown to have higher connectivity values in surface, volume and transmission than Wood biochars as well as larger pores as observed by pore size distribution. Differences in physical properties between colonised and non-colonised particles were larger in *Miscanthus* biochar than in Wood biochar.

Conclusions

Colonisation was more vigorous in Wood biochar than in *Miscanthus* biochar, even when our findings from physical pore space analysis suggest better habitat quality in *Miscanthus* biochar than in Wood biochar. We conclude that (i) the selected feedstocks display large differences in microbial habitat quality as well as in physical pore space characteristics and (ii) the physical description of biochars alone does not suffice for the reliable prediction of microbial habitat quality. Thuswe recommend that physical and surface chemical data should be linked for this purpose.

Introduction

Biochar is considered a promising means both to sequester carbon from the atmosphere and improve soil fertility (Lehmann et al. 2011). The latter is thought to be achieved by changes in soil physico-chemical properties such as pH, cation exchange capacity, and water holding capacity. In addition, recent evidence has indicated that biochar may also impact on soil microbial community structure and function (Ennis et al. 2000; Pietikäinen et al. 2000;

Quilliam et al. 2012; Weber et al. 1978). The notably large number of recent studies investigating biochar – (micro)organisms interactions, i. e. microbial responses to biochar as a soil amendment, reflects the relevance of the topic for the scientific community, but also for a climate-neutral agriculture (EBC 2012; Ennis et al. 2012; Jaafar et al. 2014; Quilliam et al. 2013). However, contradicting results have been found regarding biochars' direct impact on soil microbial communities, indicating a high specificity of every biochar and great heterogeneity within defined biochar samples in terms of physico-chemical properties influencing microbial colonisation.

The enormous diversity of feedstocks and technologies currently available for carbonisation leads to highly diverse products that vary in chemical (composition and content of elements) and physical properties (e.g. pore geometry) as well as in functions (hydrophobicity, sorption of nutrients and contaminants; Budai et al. 2014; Morales et al. 2015; Naisse et al. 2013; Riedel et al. 2014; Wiedner et al. 2013). For example, pyrolytic biochars derived from C-rich plant material under a high temperature and long processing time display a higher degree of condensation leading to greater sorption of ions in aqueous solution and possibly greater recalcitrance to decomposition processes, as compared to chars derived from animal waste at lower temperatures (Luo et al. 2013; Marchal et al. 2013; Nguyen et al. 2008).

Physical pore space characteristics and pore geometries determine the availability and accessibility of pore space habitable to microorganisms and are important parameters influencing whether a piece of biochar is subject to autochthonous colonisation processes or not (Ascough et al. 2010; Bird et al. 2008; Hattori 1988; Jaafar et al. 2014; Quilliam et al. 2013). The link between physical pore space characteristics and microbial habitat quality is given by the shape of habitat functionality as a result of porosity, physical surface area and connectivities. Whether the pores of a particle are filled with water or gaseous phase and whether water, gas, and nutrient flux between the pores occurs is key to microbial habitat quality and shaped by the investigated parameters (Spoering & Lewis 2001; Thormann et al.

2004; Willey et al. 2009). Moreover, the pore size distribution (PSD) describes which pore space is actually accessible to soil life due to size limitations (Hattori, 1988). As many microorganisms show movement which is passive by water flow rather than active motility, spread along particle surfaces is considered a major means of movement, rendering pore space characteristics such as surface or directional connectivity more meaningful to microbial colonisation than bulk parameters like porosity or physical surface area (Spoering & Lewis 2001). While surface and volume connectivity have a high relevance for microbial colonisation and interaction within the pore volume, directional connectivity characterises the accessibility of pores to entering organisms and matter fluxes in the solution, which is essential for nutrient provision to plants (Young et al. 2008).

There is broad agreement that fungal hyphae can access biochar for habitat (Ascough et al. 2010; Jaafar et al. 2014), but it is yet uncertain whether organic compounds leaching from biochars provide possible substrates both to fungi and bacteria (Koide et al. 2011). Many biochar-related studies address microbial activity and report observed effects to be a result of biochar amendment (Ennis et al. 2012; Gomez et al. 2014; Jones et al. 2011; Luo et al. 2011; Quilliam et al. 2012; Yanai et al. 2007). Most studies target functions of soil ecosystems such as C mineralisation and denitrification and related bulk parameters (trace gas evolution) are often recorded (Ameloot et al. 2013; Cayuela et al. 2013; Jones et al. 2011; Luo et al. 2011; Yanai et al. 2007). Hence, there is a gap of knowledge in mechanistically linking effects such as substrate utilisation by soil microorganisms to their actual sources and only few studies systematically target specific microorganisms, either by direct observation using microscopy or by group-specific biomarkers (Ascough et al. 2010; Jaafar et al. 2014; Pietikäinen et al. 2000; Quilliam et al. 2013; Weber et al. 1978).

Recent studies acknowledged that the diversity of soils, biochars, and autochthonous microbial communities used in studies on the subject makes it difficult to derive patterns of biochar effects both on soil properties and on soil biota (Baveye, 2014; Lehmann et al. 2011).

Therefore, it is necessary to start off with physical key properties such as porosity and its geometry for analysis and subsequently increase the level of complexity for maintaining a clear view while producing comprehensive mechanistic ideas. While surface chemical properties are certainly of importance (Kim et al. 2012; Kinney et al. 2012; Luo et al. 2013), this work exclusively focuses on physical pore space characteristics in biochars of different feedstocks and hence implications for microbial habitat quality.

We here address physical properties of two pyrolytic biochars from different feedstocks and their potential impact on microbial colonisation. We investigated spontaneous microbial colonisation as well as a fungal inoculation on each type of biochar, and used X-ray µ-CT 3D reconstructions of biochar particles as a basis for analysis of aforementioned physical properties. As biochar is a highly heterogeneous material (Bucheli et al. 2014), µ-CT offers the possibility to investigate and quantify habitat heterogeneity of believed highly defined chars, thus avoiding possibly contradicting results for the behaviour of small and very specific batches of biochar. However, in X-ray µ-CT there is a general trade-off between scan resolution and quality which can hamper subsequent scan analyses especially in samples rich in low density materials such as compost or biochar (Quin et al. 2014; Baveye et al. 2010).

We expect the biochars of two different feedstocks to be different in pore geometry for all investigated parameters. Since fungal inoculation enters biochars' pores, it is assumed that porosities would be reduced but analysed surface and directional connectivities would be increased due to the establishment of pathways via fungal growth.

Materials and methods

Biochars and treatments

Chars representing different feedstocks and being commonly applied as soil amendments were used in order to account for differences in the investigated properties. Commercial

biochars from mixed deciduous and coniferous woods (W; Schottdorf, Romania) and *Miscanthus* (M; delinat, Switzerland) chips were purchased and shipped in sealed big-bags directly after production to the University of Bremen where they were stored for 3 years in a dry shed under outdoor temperature conditions. Both biochars are of pyrolytic origin and highest treatment temperature was 700°C. Particles of 5 – 15 mm in size and of different shapes were hand-sorted (at least 100 per biochar) in order to ensure proper handling and preparation for subsequent analyses. An equivalent set of biochar particles (> 50 pieces per biochar) was selected and subjected to fungal colonisation by *Agaricus bisporus*. Biochar pieces were soaked with sterile mushroom substrate solution and inoculated with sterile *Agaricus bisporus* grain spawn (Pilzland Vertriebs GmbH, Germany) for six weeks (pers. comm. D. Grimm). Thus four treatments were defined which are differentiated by the factors of native (non-inoculated) biochars (Mn, Wn) and fungal colonised (Mf, Wf) for both feedstocks. All biochar samples were stored air dried with water contents of 3.6, 6.8, 2.4, and 4.9 % for Mn, Wn, Mf, and Wf respectively (gravimetric water content; determination based on 25 pieces each).

Microbiological analyses

A total of 60 pieces of each native biochar (Mn, Wn) were placed on sterile peptone-meat-glucose (PMG) agar plates with three pieces per plate and incubated at 28°C in the dark for 72 h. Presence or absence of colonies were recorded for each biochar particle and documented in photographs. Selected strains were isolated to single pure colonies, transferred to liquid medium and incubated overnight for bacteria and one week for fungi at 22°C in the dark on an orbital shaker with 125 rpm.

An extraction of DNA from biochars directly resulted in insufficient yields and purity for subsequent PCR-analyses. This has also been reported for biochar amended soils and charcoal (Gani et al. 1999; Leite et al. 2014). Therefore bacterial DNA was extracted from isolates and

16S rRNA genes were amplified via PCR using universal bacterial primers Gm5F (with GC clamp) and 907r (Muyzer et al. 1995). Fungal strains were selected by colony morphology and corresponding 18S rRNA genes were PCR amplified using the NS1 and EF3 primers (Hoshino & Morimoto 2008). PCR fragments were separated by denaturing gradient gel electrophoresis (DGGE) and selected bands in the fingerprints were purified and reamplified for subsequent Sanger sequencing (LGC Genomics, Germany; details are given as supplementary information). Obtained bacterial sequences were subjected to NCBI BLAST (Altschul et al. 1990) and best hits were aligned together with query sequences using the MEGA 6.0 software (Tamura et al. 2013). Phylogeny was reconstructed using the Maximum Likelihood analysis in MEGA (Tamura & Nei 1993) with *Escherichia coli* sequence as outgroup for tree rooting. Fungal sequences were classified using the Sina Alignment service of the SILVA database (Pruesse et al. 2012).

Respiration analyses of both native biochars (Mn, Wn) were done as a measure for native microbial colonisation and activity. A set of 15 pieces of biochar (same selection criteria as described above; approx. 500 mg) was selected per respiration treatment i.e. substrate induced respiration after soaking pieces of biochar in glucose solution (500 µL, 30 mg L^{-1}), basal respiration after soaking biochars in sterile water (500 µL), and biochars with their original moisture (5.4 % and 8.9 % gravimetric water content for *Miscanthus* and Wood biochar respectively). Samples were incubated at 22°C in air tight glass vials (20 mL, n = 5 per treatment) and CO_2 was analysed in the headspace after 20 hours via gas chromatography (FID with methanizer) and extrapolated to µmol CO_2 per day and dry weight of biochar.

X-ray µ-CT

X-ray µ-CT was performed using scanning facilities at the SIMBIOS Centre, Abertay University Dundee, UK (HMX ST 225, Metris X-Tek, UK). A set of six air dried biochar pieces were randomly selected per treatment (Mn, Wn, Mf, Wf) and fixed on the stage in the

CT scanner by double sided tape. Scan settings were optimised for parameters appropriate for both feedstocks and the subsequent analyses. Due to the low optical density of the material against X-rays, *Miscanthus* and Wood biochar particles were scanned at an energy of 55 kV and 50 kV respectively, a current of 190 µA, 1000 angular projections, and four frames per projection at a resolution of 5.67 µm per voxel. Radiographs were reconstructed into a three-dimensional volume using CT-Pro v.1.6 (NIKON Metrology, UK).

Image processing and pore space analyses

3D volume datasets were processed in VGStudio Max 2.0 (Volume Graphics, Germany) for grey-scale enhancement and exported as 2D 8-bit BMP image stacks. Regions of interest (ROI) were selected with ImageJ/Fiji software (Schindelin et al. 2012) and cropped to cubes of 128^3 volumetric pixels (voxels) in order to ensure that their location is completely within the particle volume. Grey-scale image stacks were segmented into binary images using the fully automated Adaptive Window Indicated Kriging algorithm (Houston et al. 2013a). Porosity, surface area, and connectivities were calculated with in-house developed algorithms for Minkowski Functionals and connectivity analysis (Baveye et al. 2010; Hapca et al. 2013; Houston et al. 2013b). The latter was analysed as volume connectivity (VC) and surface connectivity (SC) describing the probability that two pore voxels or pore-solid interfaces are connected respectively. The directional connectivity (DirC) is a measure for the probability that two randomly chosen points on the opposite surface of the ROI cube are connected via pores.

For the pore size distribution (PSD) image stacks were processed using ImageJ/Fiji plugin „BoneJ“ (Doube et al. 2010) modified by A. Houston (SIMBIOS Centre, Abertay University Dundee). This plug-in calculates the PSD from local thickness maps using the Maximum Inscribed Balls method (Hildebrand & Ru 1997; Xie et al. 2006; Dougherty & Kunzelmann 2007; Liao 2014). A total of six particles per treatment and five individual ROIs per particle

were analysed (Figure 1). As the selected ROIs per particle are assumed to be independent of particle size and identity, a sample size of n = 30 ROIs was obtained for each of the four treatments.

Figure 1

Statistical analyses

All statistical tests were performed within the R environment (R core project 2013). Presence and absence data of emerged colonies were analysed using Welch's two-sided t-test to determine significant differences in biochar feedstocks. Respiration data were sqrt transformed for normality and analysed with a multifactorial ANOVA followed by a Tukey HSD post-hoc test to analyse the effect of biochar feedstock and substrate addition on CO_2 production after 24 h. All data related to surface and volume properties were log transformed for normality and analysed with a multifactorial ANOVA followed by a Tukey HSD post-hoc test to analyse the effect of biochar feedstock and fungal colonisation on porosity, physical surface area, and connectivity. To investigate the effect of the different biochar treatments on PSD, a two-parameter gamma distribution model was fitted to the PSDs obtained for the biochar samples. The Non-Linear Mixed-Effect procedure in R (nmle package in R v.3.1.1) was used to fit the gamma distribution to the data and to investigate significant difference in the PSD model parameters estimated for the different treatments. Data were first grouped per sample, then the two factors, biochar type (with levels W and M) and fungal inoculation (with levels present-f and absent-n) were introduced in the model and investigated for significant main and interaction effects giving a total of four treatments with six replicates per treatment. The samples were introduced as random factor in the model.

Results

Microbiological analyses

Microbial growth from particles of both biochars was widely dominated by extensive mycelial formations. While colonies were emerging from 93.3 % of the Wood biochar particles, colonies emerged only from 30.0 % of the *Miscanthus* biochar particles ($p < 0.001$). Bacterial colonies from Wood biochar proliferated faster than colonies from *Miscanthus* biochar which emerged with delay (up to 72 hours). In average colonies emerged from *Miscanthus* biochar were 4.8 times smaller than from Wood biochar (45.1 ± 13.7 mm² and 216.9 ± 69.5 mm² respectively) after 72 hours incubation and were less diverse.

Sanger sequencing of isolates revealed 13 bacterial sequences of which five were isolated from cultures on *Miscanthus* biochar and eight from Wood biochar. All identified strains belong to the gram-positive bacteria with 12 strains clustering within the *Bacillales* order of Firmicutes (low-GC group) and one strain clustering within the *Actinomycetales* order of Actinobacteria (high-GC group). Identified strains were exclusively found on the same type of biochar, but no particular pattern of biochar-specific phylogenetic clustering was observed (Figure 2). Three fungal isolates from Wood biochar were identified via sequencing. Two of the sequences belong to the Ascomycota group of fungi and were identified as *Penicillium* and *Coniochaeta* and the third one and was identified as *Mucor* which belongs to the Zygomycota group of fungi.

Figure 2

For microbial respiration a significant interaction between both factors, biochar feedstock and substrate, was observed ($p < 0.05$, Figure 3). Least differences occurred between the two feedstocks for basal respiration of air dry samples. In *Miscanthus* biochar, water addition did not significantly alter CO_2 evolution and only glucose addition lead to a significant increase in

261 CO_2 production compared to the air dry stage. In Wood biochar respiration significantly
262 increased following water saturation and subsequent glucose addition. No significant
263 differences were observed for basal respirations between water saturated *Miscanthus* and dry
264 Wood biochar or between substrate induced respiration of *Miscanthus* and water saturated
265 basal respiration of Wood biochar.
266
267 Figure 3
268
269 ***X-ray µ-CT analyses***
270 Applying optimised scan settings, we were able to resolve both biochars' physical structures
271 and successfully applied automated thresholding methods enabling subsequent pore space
272 analysis. Apart from pore space and biochar matrix, indications of fungal colonisation were
273 resolved as a region of higher optical density ranging from the particle surface to the centre in
274 sliced CT images (Figure 4A). Thresholded images of selected regions of interest (ROIs)
275 revealed differences in shape and orientation of pores in 2D slices (Figure 4B) and 3D
276 reconstructions thereof (Figure 4C).
277 No systematic effect of the biochar and fungal inoculation on porosity was found ($p > 0.05$,
278 Figure 5). However, a significant interaction between the two factors was observed ($p < 0.05$).
279 The post-hoc test revealed significant differences ($p < 0.05$) between both native biochars. For
280 the treatments inoculated with fungi no significant differences were observed between the two
281 biochars. In Wood biochar fungal inoculation showed a slight trend towards higher porosity
282 (+ 1.6 %) and the porosity of *Miscanthus* biochar colonised with fungi was significantly
283 decreased by 2.3 %.
284 Similar physical surface areas (PSA) were analysed for both biochars which was 144.6 µm²
285 and 137.4 µm² per ROI cube (± 5.6 µm² and ± 7.7 µm², $n = 30$) for *Miscanthus* and Wood

biochar respectively (Figure 6). Concerning PSA, only fungal colonisation was found to exert a significant ($p < 0.001$) influence, diminishing PSA by approximately 20 % in both biochars.

Figure 4

Both biochar feedstock and fungal inoculation were found to be significant for all analysed types of connectivity and a significant interaction was found between the two factors (Figure 7). *Miscanthus* biochar displayed higher connectivities (0.16 for surface connectivity (SC) in Mn and 0.04 in Mf, 0.21 for volume connectivity (VC) in Mn and 0.05 in Mf, and 0.63 for directional connectivity (DirC) in Mn and 0.44 in Mf) than Wood biochar (0.05 for SC in Wn and Wf, 0.07 for VC in Wn and 0.06 in Wf, and 0.36 for DirC in Wn and 0.46 in Wf) regardless whether fungal inoculation was applied or not. However, fungal inoculation was significant only in *Miscanthus* biochar, but not in Wood biochar. Without fungal inoculation both types of biochar displayed different connectivity, which disappeared with fungal colonisation.

Figure 5

Figure 6

Figure 7

There was no significant difference in pore size distribution (PSD) between the two biochars alone (gamma parameters $p > 0.05$). However, a significant interaction was found between biochar type and fungal inoculation (scale parameter $p < 0.05$), indicating a biochar-specific effect of fungal colonisation on PSD. Only in Wood biochar fungal colonisation was found to be significant, with larger pores in colonised particles, while no significant difference between

native and fungi inoculated particles occurred in *Miscanthus* biochar (gamma parameters $p > 0.52$) (Figure 8).

Figure 8

Discussion

From a microbial perspective, pore space and pore surface properties of biochar are the main determinants for physical habitat quality as they represent the actual physical habitat. Especially the connectivities of pores are of importance as they determine the accessibility of pores to microorganisms and aqueous, nutrient containing solutions crucial to microbial life (Young et al. 2008).

With optimised scan settings for the X-ray µ-CT, reconstructed biochar structure could be visualised at a high resolution of 5.67 µm per voxel for two different, low density materials, i. e. Wood biochar and *Miscanthus* biochar particles. As a result of thresholding algorithm and pore space identification pores larger than the scan resolution are considered for further analyses. Consequently, only pores larger than two voxels (11.34 µm) are recognised in PSD calculation. As the smallest recorded pore diameter was 12.01 µm in Wood biochar and 12.46 µm in *Miscanthus* biochar, the micro- and nanopore fraction, which possibly represents a large portion of total porosity (up to <80%; Gray et al. 2014) is naturally omitted here. However, our analyses are conducted on a scale relevant for the assessment of microbial habitat quality as many microorganisms have a diameter below the pore sizes detected in this study (Hattori 1988). Also, proliferation of fungal inoculates was concluded due to higher densities of biochars' matrix in the µ-CT scans. Fungal colonisation of pores was confirmed via scanning electron microscopy and appeared on the edges of biochar particles showing dense surface colonisation and access of exposed tube-like pores (supplementary information Figure S1). Due to the high similarity in optical density between biochar and the mycelium no

quantification of fungal biomass or habitat access was possible. Nevertheless, changes in functional pore space characteristics between biochar colonised by fungi and native biochar particles is indicative of extensive habitat access by the fungus.

Our microbiological approach of testing bacterial presence on the biochars' surface was influenced by mycelial structures on the agar plates which proliferated much faster than emerging bacterial colonies. However, fungal habitat potential of the two biochars is accounted for by the indication of fungal hyphae in the biochar particles via X-ray µ-CT and the related changes in pore space characteristics..

We did not find differences between Wood and *Miscanthus* biochar regarding porosity or physical surface area as determinants of habitable space available for microbial colonisation. However, the significant interactions between biochar and fungal inoculation throughout the analyses indicate biochar-specific colonisation patterns. Moreover, differences between the biochars were significant for the “functional” parameters of connectivities in surface, volume and direction, and pore size distribution. *Miscanthus* biochar displayed higher connectivity values and larger pores (by PSD) than Wood biochar. Furthermore, analysis of variance showed that Wood biochar was more homogeneous than *Miscanthus* biochar, despite wood itself being a much more heterogeneous material than grass fibres and its composition from both deciduous and coniferous species. It is possible that wood has a higher thermo-mechanical stability of macrostructure than *Miscanthus*, leading to more pyrolysis-induced cracks in *Miscanthus* biochar and rendering the latter more heterogeneous (Pattanotai et al. 2014; Zhang et al. 2013b; Demirbas 2004). This was observed in exemplary tests via scanning electron microscopy as well, where clear differences in surface and internal structure of the investigated biochars could be shown (Figure 9).

Figure 9

With larger pores and higher connectivities, *Miscanthus* biochar would be expected to represent better habitat than Wood biochar. However, our results both from X-ray µ-CT and microorganism isolation suggest the contrary. The significant interaction between biochar and fungal colonisation in surface connectivity ($p = 0.007$) as well as in volume connectivity ($p = 0.009$) and PSD ($p < 0.05$) indicates biochar-specific proliferation of the fungal inoculate with better growth in Wood biochar than in *Miscanthus* biochar. These findings are in line with results from other studies describing intense wood biochar colonisation by saprophytic fungi (Ascough et al. 2010; Jaafar et al. 2014). Additional studies describe beneficial effects of wood derived biochar on saprophytic fungi to occur only after ≥ 60 days of soil incorporation (Gul et al. 2015). Microorganisms' preference of Wood biochar over *Miscanthus* biochar is supported by findings from our isolation experiment with almost all (94 %) Wood biochar particles shown to harbour bacteria, which was the case for less than a third (30 %) of all tested *Miscanthus* biochar particles.

We have no notion of studies addressing direct observation of microbial colonisation on *Miscanthus* biochar. However, as physical bulk parameters such as porosity and surface area were not different from Wood biochar, we suggest that surface chemical properties, such as hydrophobicity, functionality, and surface charge, exert a strong selective influence on microbial attachment on the biochar surface. Hydrophobicity is frequently observed in biochars produced at high temperatures and is a result of increased C condensation and, consequently, reduced surface functionality (Gray at al. 2014). It is known that hydrophobic / hydrophilic interactions strongly determine water adsorption to surfaces which in turn affects bacterial adhesion. Zhang et al. (2003a) showed that bacterial adhesion was reduced by using superhydrophobic surfaces. Similar mechanisms may apply for bacteria attached on biochar surfaces, but further research is needed to confirm that hydrophobicity is the main adverse agent of bacterial adhesion in *Miscanthus* biochars.

Naturally, our approach of placing biochar particles on agar plates and investigating emerging colonies is constraint by the limited contact surface (less than 50% of the particles' surface) between the biochar particles and the medium. However, assuming all parts of a biochar particle have the same probability of exposure towards microbial colonisation, our partial insights can be regarded as representative for the entire biochar particles. Nevertheless, oligotrophic microorganisms are substantially neglected using a standard nutrient medium for cultivation as we did (Atlas 2010).

Remarkably, the vast majority of isolated bacteria belonged to the *Bacillales* order of Firmicutes, also known as the low-GC group of gram-positive bacteria. While hardly motile, this group is known to form biofilms of high cellular density and mechanical stability (Simões et al. 2007), sometimes even displaying mycelial structures as in the case of *Paenibacillus* (Willey et al. 2009). The results obtained in the respiration experiment and performed with a single and non-complex nutrient source are supportive for the findings of distinct bacterial communities on the surface of biochars with distinct properties. Our results again indicate much more active communities on the Wood biochar than on the *Miscanthus* biochar.

While the biochar itself probably exerts a selective influence on microbial attachment and colonisation, it must not be neglected that every colonisation reflects the materials' exposure history e.g. during quenching with water after pyrolysis as a further selective factor. As both biochars were stored under the same conditions, they either exert a very strong selective influence on their spontaneous colonisation or have been exposed to colonisation between pyrolytic production and packing. Either case is important for practitioners because biochars can act as vectors for the distribution of microorganisms (Kim et al. 2012).

The high abundance of microorganisms isolated suggests the presence of numerous cells on the surface of commercially available, non-activated biochar and that this material can by no means be regarded sterile. However, as respiration analysis revealed these organisms are hardly active on the biochar surface or merely persist as endospores. It also remains

undiscovered whether these spontaneous colonisers are of significance during biochar activation or are outcompeted upon incorporation into the soil matrix (Abiven et al. 2007). For further mechanistic insight studies must pin-point the identity and activity of microorganisms on the biochar surface and link both to the material's exposure history. Little is known also about distinct physico-chemical features of different pore size classes in biochars and their implications for microbial colonisation although there may be many. More important for the conception of optimal biochar activation and amendment to soil will be the investigation of soil-borne microorganisms and their role in biochar incorporation into the soil matrix. This question is of particular practical relevance as microbial colonisation exerts a great influence on soil aggregation which is changed in patterns by biochar amendment (Abiven et al. 2007; Ouyang et al. 2013).

Conclusion

Biochar physical properties influence microbial habitat quality by regulating water flow, nutrient exchange, and space accessible to colonising organisms. We showed that physical properties of biochar vary with feedstocks used for pyrolysis. Biochar derived from *Miscanthus* has a tendency towards larger pores and higher connectivities than Wood biochar. While Wood biochar is a rather homogeneous material, biochar derived from the grass *Miscanthus* displays a higher variability, probably due to low mechanical stability and subsequent breaking. But habitat features such as porosity, physical surface area, and pore size distribution can be influenced by colonising organisms, as access by fungal hyphae shows. This renders habitat quality as a dynamic feature, prone to constant change as colonisation takes place.

We also revealed bacterial presence on the biochar surface to be biochar-specific. Rapidly developing colonies were found to emerge from Wood biochar compared to *Miscanthus*

biochar. However, bacteria identity did not follow any biochar-specific pattern as all isolated bacteria belong to the gram-positive bacteria with most representing the *Bacillales* order and one sequence belonging to the *Actinomycetales* order.

For enhanced practical relevance of the subject further insight is needed into the activity patterns of soil microorganisms on the biochar surface and the factors driving microbial colonisation of biochars both during activation and after incorporation into the soil environment. Especially further insight into (chemical) surface properties of biochars derived from various feedstocks will be promising in order to design biochars with distinct physico-chemical properties for specific purposes and applications.

Acknowledgment

The X-ray µ-CT analyses were carried out by LS at Abertay University, Dundee, UK as part of a short term scientific mission funded by the COST Action Biochar TD1107. Both the COST Action Biochar and the SIMBIOS Centre at Abertay University are acknowledged for funding and hosting respectively. Special Thanks is given to Sonja Schmidt and Ruth Falconer for technical assistance in µ-CT scanning and to Alasdair Houston for provision and assistance with image processing algorithms. Daniel Grimm is acknowledged for provision of fungal inoculated biochars and Ingo Dobner for kind provision of non-colonised biochars.

References

Abiven S, Menasseri S, Angers DA, Leterme P (2007) Dynamics of aggregate stability and biological binding agents during decomposition of organic materials. European Journal of Soil Science, 58(1), 239–247.

Altschul SF, Gish W, Miller W, Myers EW, Lipman DJ (1990) Basic local alignment search tool. Journal of Molecular Biology, 215, 403–410.

Ameloot N, De Neve S, Jegajeevagan K, Yildiz G, Buchan D, Funkuin YN, Nkwain Fukuin Y, Prins W, Bouckaert, L, Sleutel, S (2013) Short-term CO_2 and N_2O emissions and microbial properties of biochar amended sandy loam soils. Soil Biology and Biochemistry, 57, 401–410.

Ascough PL, Sturrock CJ, Bird MI (2010) Investigation of growth responses in saprophytic fungi to charred biomass. Isotopes in Environmental and Health Studies, 46, 64–77.

Atlas RM (2010) Handbook of Microbiological Media. Fourth Edition. CRC Press.

Baveye PC (2014) The biochar dilemma. Soil Science Society of America Journal, 52(3), 217.

Baveye PC, Laba M, Otten W, Bouckaert L, Dello Sterpaio P, Goswami RR, Grinev D, Houston A, Hu Y, Liu J, Mooney S, Pajor R, Sleutel S, Tarquis A, Wang W, Wei Q, Sezgin M (2010) Observer-dependent variability of the thresholding step in the quantitative analysis of soil images and X-ray microtomography data, 51–63.

Bird MI, Ascough PL, Young IM, Wood CV, Scott AC (2008) X-ray microtomographic imaging of charcoal. Journal of Archaeological Science, 35(10), 2698–2706.

Bucheli TD, Bachmann HJ, Blum F, Bürge D, Giger R, Hilber I, Keita J, Leifeld J, Schmidt HP (2014) On the heterogeneity of biochar and consequences for its representative sampling. Journal of Analytical and Applied Pyrolysis, 107, 25–30.

Budai A, Wang L, Gronli M, Strand LT, Antal MJ, Abiven S, Dieguez-Alonso A, Anca-Couce A, Rasse DP (2014) Surface properties and chemical composition of corncob and *Miscanthus* biochars: Effects of production temperature and method. Journal of Agricultural and Food Chemistry, 62, 3791–3799.

488 Cayuela ML, Sánchez-Monedero MA, Roig A, Hanley K, Enders A, Lehmann J (2013)
489 Biochar and denitrification in soils: when, how much and why does biochar reduce N_2O
490 emissions? Scientific Reports, 3 (Experiment 2), 1732.

491 Demirbas, A (2004) Effects of temperature and particle size on bio-char yield from pyrolysis
492 of agricultural residues. Journal of Analytical and Applied Pyrolysis, 72(2), 243–248.

493 Doube M, Klosowksi MM, Arganda-Carreras I, Cordelières FP, Dougherty RP, Jackson JS,
494 Schmid B, Hutchinsin JR, Shefelbine SJ (2010) BoneJ. UKPMC Funders Group.

495 Dougherty R, Kunzelmann KH (2007) Computing local thickness of 3D structures with
496 ImageJ. Microscopy and Microanalysis, 13(S02), 1678–1679.

497 EBC (2012) Guidelines for a sustainable production of biochar (No. 4.8). Arbaz, Switzerland.
498 Retrieved from http://www.european-biochar.org/en/download

499 Ennis CJ, Evans AG, Islam, M, Ralebitso-Senior TK, Senior E (2012) Biochar: Carbon
500 Sequestration, Land Remediation, and Impacts on Soil Microbiology. Critical Reviews in
501 Environmental Science and Technology, 42(22), 2311–2364.

502 Gani SA, Mukherjee DC, Chattoraj DK (1999) Adsorption of biopolymer at solid-liquid
503 interfaces. 1. affinities of DNA to hydrophobic and hydrophilic solid surfaces. Langmuir,
504 15, 7130-7138.

505 Gomez JD, Denef K, Stewart CE, Zheng J, Cotrufo MF (2014) Biochar addition rate
506 influences soil microbial abundance and activity in temperate soils. European Journal of
507 Soil Science, 65, 28–39.

508 Gray M, Johnson MG, Dragila MI, Kleber M (2014) Water uptake in biochars: The roles of
509 porosity and hydrophobicity. Biomass and Bioenergy, 61, 196–205.

510 Gul S, Whalen JK, Thomas BW, Sachdeva V, Deng H (2015) Physico-chemical properties
511 and microbial responses in biochar-amended soils: Mechanisms and future directions.
512 Agriculture, Ecosystems & Environment, 206, 46–59.

513 Hapca S, Houston A, Otten W, Baveye P (2013) New local segmentation method for 3D
514 images of natural porous media, based on minimizing the intraclass grayscale variance,
515 Vandose Zone Journal, 12(1).

516 Hardie M, Clothier B, Bound S, Oliver G, Close D (2014) Does biochar influence soil
517 physical properties and soil water availability? Plant and Soil, 376, 347–361.

518 Hattori T (1988) Soil aggregates as microhabitats of microorganisms. Rep. Inst. Agric.
519 Tohoku Univ., 37, 23–36.

520 Hildebrand T, Rüegsegger P (1997) A new method for the model-independent assessment of
521 thickness in three-dimensional images, Journal of Miscroscopy, 185, 67–75.

522 Hoshino YT, Morimoto S (2008) Comparison of 18S rDNA primers for estimating fungal
523 diversity in agricultural soils using polymerase chain reaction-denaturing gradient gel
524 electrophoresis. Soil Science and Plant Nutrition, 54(5), 701–710.

525 Houston AN, Otten W, Baveye PC, Hapca S (2013a) Adaptive-window indicator kriging. A
526 thresholding method for computed tomography images of porous media. Computers and
527 Geosciences, 54, 239–248.

528 Houston AN, Schmidt S, Tarquis AM, Otten W, Baveye PC, Hapca SM (2013b) Effect of
529 scanning and image reconstruction settings in X-ray computed microtomography on
530 quality and segmentation of 3D soil images. Geoderma, 207-208, 154–165.

531 Jaafar NM, Clode PL, Abbott LK (2014) Microscopy observations of habitable space in
532 biochar for colonization by fungal hyphae from soil. Journal of Integrative Agriculture,
533 13(3), 483–490.

534 Jones DL, Murphy DV, Khalid M, Ahmad W, Edwards-Jones G, DeLuca TH (2011) Short-
535 term biochar-induced increase in soil CO_2 release is both biotically and abiotically
536 mediated. Soil Biology and Biochemistry, 43(8), 1723–1731.

537 Kim P, Johnson AM, Essington ME, Radosevich M, Kwon WT, Lee SH, Rials TG, Labbé N
538 (2012) Effect of pH on surface characteristics of switchgrass-derived biochars produced
539 by fast pyrolysis. Chemosphere, 90(10), 2623–2630.

540 Kinney TJ, Masiello CA, Dugan B, Hockaday WC, Dean MR, Zygourakis K, Barnes RT
541 (2012) Hydrologic properties of biochars produced at different temperatures. Biomass
542 and Bioenergy, 41, 34–43.

543 Koide RT, Petprakob K, Peoples M (2011) Quantitative analysis of biochar in field soil. Soil
544 Biology and Biochemistry, 43(7), 1563–1568.

545 Lehmann J, Rillig MC, Thies J, Masiello CA, Hockaday WC, Crowley D (2011) Biochar
546 effects on soil biota – A review. Soil Biology and Biochemistry, 43(9), 1812–1836.

547 Leite DCA, Balieiro FC, Pires CA, Madari BE, Rosado AS, Coutinho HLC, Peixoto RS
548 (2014) Comparison of DNA extraction protocols for microbial communities from soil
549 treated with biochar. Brazilian Journal of Microbiology, 45, 175-183.

550 Liao Z, Zeyuan A-Z, Orecchia L (2014) Using optimization to find maximum inscribed balls
551 and minimum enclosing balls. ArXiv:1412.1001 [cs.CG]

552 Luo Y, Durenkamp M, De Nobili M, Lin Q, Brookes PC (2011) Short term soil priming
553 effects and the mineralisation of biochar following its incorporation to soils of different
554 pH. Soil Biology and Biochemistry, 43(11), 2304–2314.

555 Luo Y, Durenkamp M, De Nobili M, Lin Q, Devonshire BJ, Brookes PC (2013) Microbial
556 biomass growth, following incorporation of biochars produced at 350 °C or 700 °C, in a
557 silty-clay loam soil of high and low pH. Soil Biology and Biochemistry, 57, 513–523.

558 Marchal G, Smith KEC, Rein A, Winding A, Trapp S, Karlson UG (2013) Comparing the
559 desorption and biodegradation of low concentrations of phenanthrene sorbed to activated
560 carbon, biochar and compost. Chemosphere, 90(6), 1767–1778.

561 Morales VL, Perez-Reche FJ, Hapca SM, Hanley KL, Lehmann J, Zhang W (2015) Reverse
562 engineering of biochar. Bioresource Technology, 183, 163-174.

563 Muyzer G, Teske A. Wirsen CO, Jannasch HW (1995) Phylogenetic relationships of
564 *Thiomicrospira* species and their identification in deep-sea hydrothermal vent samples
565 by denaturing gradient gel electrophoresis of 16S rDNA fragments. Archives of
566 microbiology, 164, 165-172.

567 Naisse C, Alexis M, Plante A, Wiedner, K, Glaser B, Pozzi A, Carcaillet C, Criscuoli I,
568 Rumpel, C. (2013). Can biochar and hydrochar stability be assessed with chemical
569 methods? Organic Geochemistry, 60, 40–44.

570 Nguyen BT, Lehmann J, Kinyangi J, Smernik R, Riha SJ, Engelhard MH (2008) Long-term
571 black carbon dynamics in cultivated soil. Biogeochemistry, 92(1-2), 163–176.

572 Ouyang L, Wang F, Tang J, Yu L, Zhang R (2013) Effects of biochar amendment on soil
573 aggregates and hydraulic properties. Journal of Soil Science and Plant Nutrition, 13(4),
574 991–1002.

575 Pattanotai T, Watanabe H, Okazaki K (2014) Gasification characteristic of large wood chars
576 with anisotropic structure. Fuel, 117, 331–339.

577 Pietikäinen J, Kiikkilä O, Fritz H (2000) Charcoal as a habitat for microbes and its effect on
578 the microbial, OIKOS, 89, 231–242.

579 Pruesse E, Peplies J, Glöckner FO (2012) SINA: accurate high-throughput multiple sequence
580 alignment of ribosomal RNA genes. Bioinformatics (Oxford, England), 28(14), 1823–9.

581 Quilliam RS, Glanville HC, Wade SC, Jones DL (2013) Life in the `charosphere' - Does
582 biochar in agricultural soil provide a significant habitat for microorganisms? Soil
583 Biology and Biochemistry, 65, 287–293.

584 Quilliam RS, Marsden KA, Gertler C, Rousk J, DeLuca TH, Jones DL (2012) Nutrient
585 dynamics, microbial growth and weed emergence in biochar amended soil are influenced
586 by time since application and reapplication rate. Agriculture, Ecosystems &
587 Environment, 158, 192–199.

588 Quin PR, Cowie AL, Flavel RJ, Keen BP, Macdonald LM, Morris SG, Singh BP, Young
589 IM,Van Zwieten L (2014) Oil mallee biochar improves soil structural properties—A
590 study with x-ray micro-CT. Agriculture, Ecosystems and Environment, 191, 142–149.

591 R core project (2013) R project. Vienna. Retrieved from http://www.r-project.org/

592 Riedel T, Iden S, Geilich J, Wiedner K, Durner W, Biester H (2014) Changes in the molecular
593 composition of organic matter leached from an agricultural topsoil following addition of
594 biomass-derived black carbon (biochar). Organic Geochemistry, 69, 52–60.

595 Schindelin J, Arganda-Carreras I, Frise E, Kaynig V, Longair M, Pietzsch T, Preibisch S,
596 Rueden C, Saalfeld S, Schmid B, Tinevez JY, White DJ, Hartenstein V, Eliceiri K,
597 Tomancak P, Cardona A (2012) Fiji: an open-source platform for biological-image
598 analysis. Nat Meth 9, 676-682.

599 Simões M, Cleto S, Pereira MO, Vieira MJ (2007) Influence of biofilm composition on the
600 resistance to detachment. Water Science and Technology, 55, 473–480.

601 Spoering AL, Lewis K (2001) Biofilms and planktonic cells of Pseudomonas aeruginosa have
602 similar resistance to killing by antimicrobials. Journal of Bacteriology, 183, 6746–6751.

603 Tamura K, Nei M (1993) Estimation of the Number of Nucleotide Substitutions in the Control
604 Region of Mitochondrial DNA in Humans and Chimpanzees. Molecular Biology and
605 Evolution, 10(3) 512–526.

606 Tamura K, Stecher G, Peterson D, Filipski A, Kumar S (2013) MEGA6: Molecular
607 evolutionary genetics analysis version 6.0. Molecular Biology and Evolution, 30(12),
608 2725–2729.

609 Thormann KM, Shukla S, Pelletier DA, Spormann AM (2004) Initial phases of biofilm
610 formation in *Shewanella oneidensis* MR-1. Journal of Bacteriology, 186(23), 8096–
611 8104.

612 Weber, W, Pirbazari M, Melson G (1978) Biological growth on activated carbon: an
613 investigation by scanning electron microscopy. Environmental Science & Technology,
614 12(7), 817–819.

615 Wiedner K, Rumpel C, Steiner C, Pozzi A, Maas R, Glaser B (2013) Chemical evaluation of
616 chars produced by thermochemical conversion (gasification, pyrolysis and hydrothermal
617 carbonization) of agro-industrial biomass on a commercial scale. Biomass and
618 Bioenergy, 59, 264–278.

619 Willey JM, Sherwood LM, Woolverton C J (2009) Prescott's Principles of Microbiology.
620 Watnick, New York.

621 Xie Y, Snoeyink J, Xu J (2006) Efficient algorithm for approximating maximum inscribed
622 sphere in high dimensional polytope. Proceedings of the twenty-second annual
623 symposium on Computational Geometry, 21–29.

624 Yanai Y, Toyota K, Okazaki M (2007) Effects of charcoal addition on N_2O emissions from
625 soil resulting from rewetting air-dried soil in short-term laboratory experiments. Soil
626 Science and Plant Nutrition, 53(2), 181–188.

627 Young IM, Crawford JW, Nunan N, Otten W, Spiers A (2008) Microbial Distribution in
628 Soils: Physics and Scaling. Advances in Agronomy, 100, 81-121.

629 Zhang X, Wang L, Levanen E (2013a) Superhydrophobic surfaces for the reduction of
630 bacterial adhesion. RSC Advances 3, 12003-12020.

631 Zhang Z, Yani S, Zhu M, Li J, Zhang D (2013b) Effect of temperature and heating rate in
632 pyrolysis on the yield , structure and oxidation reactivity of pine sawdust biochar. In:
633 Chemeca 2013: challenging tomorrow. Conference paper 30430 (7 pp.).

Figure captions

Figure 1.

Experimental setup for X-ray µ-CT scanning. Particles of Wood (W) and *Miscanthus* (M) biochar with (f) and without (n) fungal colonisation are scanned and recorded 2D projections are used for 3D reconstruction. *n* (particles per treatment) = 6; *n* (ROIs per treatment) = 30.

Figure 2.

Maximum likelihood phylogeny of bacterial strains isolated from the two biochars. L#: band excised from DGGE gel; type of biochar is given in parenthesis, Mn: native *Miscanthus* biochar, Wn: native Wood biochar.

Figure 3.

Respiration of Miscanthus and Wood biochars at 22°C and three treatments. Light grey: Basal respiration of air dried biochar; Grey: Basal respiration of wet biochar; Dark grey: substrate induced respiration. Letters indicate significant differences ($p < 0.05$.); error bars: standard error, *n* = 5 replicates with 3 particles each were incubated per type of biochar and respiration treatment.

Figure 4.

Exemplary X-ray µ-CT images of biochar. (A) CT scans as visual transects through the particles; Mn: *Miscanthus* non-colonised; Mf: *Miscanthus* fungi colonised; Wn: Wood non-colonised; Wf: Wood fungi colonised. Scale bar: 500 µm. (B) Cropped images of 128 x 128 voxels at a resolution of 5.67 µm per voxel. Grey scale and corresponding thresholded image. (C) 3D reconstructions of thresholded pore space of Wood (Wn) and *Miscanthus* biochar (Mf). (D) Individual connected pore selected from 3D reconstructions (C).

Figure 5.

Porosity of the two biochars per treatment. W: Wood biochar, M: Miscanthus biochar, n: native biochar, f: fungi colonised biochar. Letters indicate significant differences ($p < 0.05$.); error bars: standard error, $n = 30$.

Figure 6.

Physical surface area (PSA) of the two biochars per treatment. W: Wood biochar, M: *Miscanthus* biochar, n: native biochar, f: fungi colonised biochar. Letters indicate significant differences ($p < 0.05$.); error bars: standard error, $n = 30$.

Figure 7.

Connectivities of the two bicohars per treatment. Dark grey: Surface connectivity (SC); Grey: Volume connectivity (VC); Light grey: Directional connectivity (DirC). W: Wood biochar, M: *Miscanthus* biochar, n: native biochar, f: fungi colonised biochar. Letters indicate significant differences ($p < 0.05$.); error bars: standard error, $n = 30$.

Figure 8.

Observed and fitted gamma distribution of the pore size distribution (PSD) of the two biochars per treatment. W: Wood biochar, M: *Miscanthus* biochar, n: native biochar, f: fungi colonised biochar.

Figure 9.

Exemplary scanning electron microscopy (SEM) images of the two biochars (non-colonised). (A) Particle overview; scale bar: 500 µm. (B) Detailed image of the particle surface. Scale bar: 100 µm. (C) Transect through the particles. Scale bar: 100 µm.

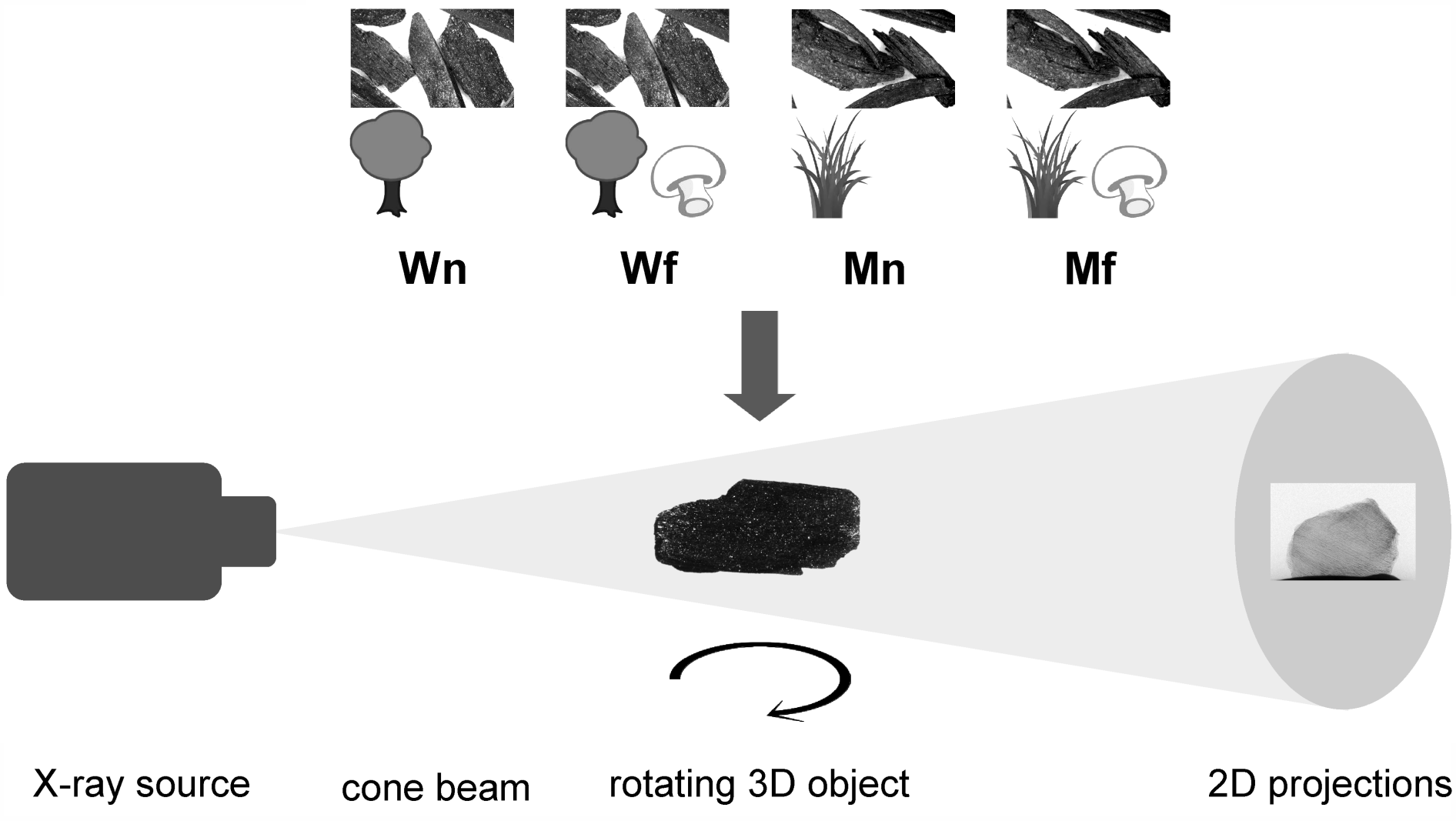
Wn
Wf
Mn
Mf
X-ray source
cone beam
rotating 3D object
2D projections

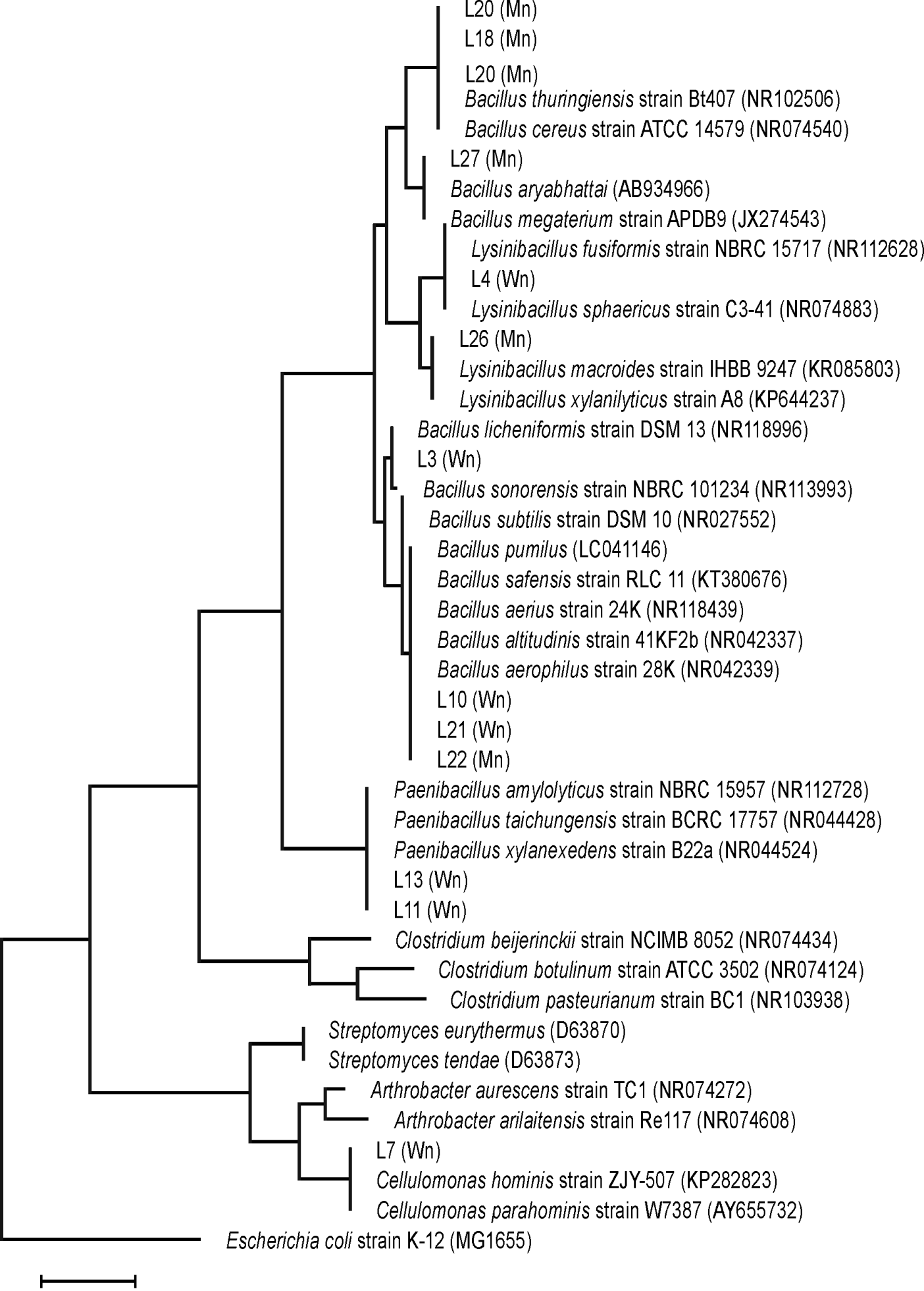
L20 (Mn)
L18 (Mn)
L20 (Mn)
Bacillus thuringiensis strain Bt407 (NR102506)
Bacillus cereus strain ATCC 14579 (NR074540)
L27 (Mn)
Bacillus aryabhattai (AB934966)
Bacillus megaterium strain APDB9 (JX274543)
Lysinibacillus fusiformis strain NBRC 15717 (NR112628)
L4 (Wn)
Lysinibacillus sphaericus strain C3-41 (NR074883)
L26 (Mn)
Lysinibacillus macroides strain IHBB 9247 (KR085803)
Lysinibacillus xylanilyticus strain A8 (KP644237)
Bacillus licheniformis strain DSM 13 (NR118996)
L3 (Wn)
Bacillus sonorensis strain NBRC 101234 (NR113993)
Bacillus subtilis strain DSM 10 (NR027552)
Bacillus pumilus (LC041146)
Bacillus safensis strain RLC 11 (KT380676)
Bacillus aerius strain 24K (NR118439)
Bacillus altitudinis strain 41KF2b (NR042337)
Bacillus aerophilus strain 28K (NR042339)
L10 (Wn)
L21 (Wn)
L22 (Mn)
Paenibacillus amylolyticus strain NBRC 15957 (NR112728)
Paenibacillus taichungensis strain BCRC 17757 (NR044428)
Paenibacillus xylanexedens strain B22a (NR044524)
L13 (Wn)
L11 (Wn)
Clostridium beijerinckii strain NCIMB 8052 (NR074434)
Clostridium botulinum strain ATCC 3502 (NR074124)
Clostridium pasteurianum strain BC1 (NR103938)
Streptomyces eurythermus (D63870)
Streptomyces tendae (D63873)
Arthrobacter aurescens strain TC1 (NR074272)
Arthrobacter arilaitensis strain Re117 (NR074608)
L7 (Wn)
Cellulomonas hominis strain ZJY-507 (KP282823)
Cellulomonas parahominis strain W7387 (AY655732)
Escherichia coli strain K-12 (MG1655)
0.05

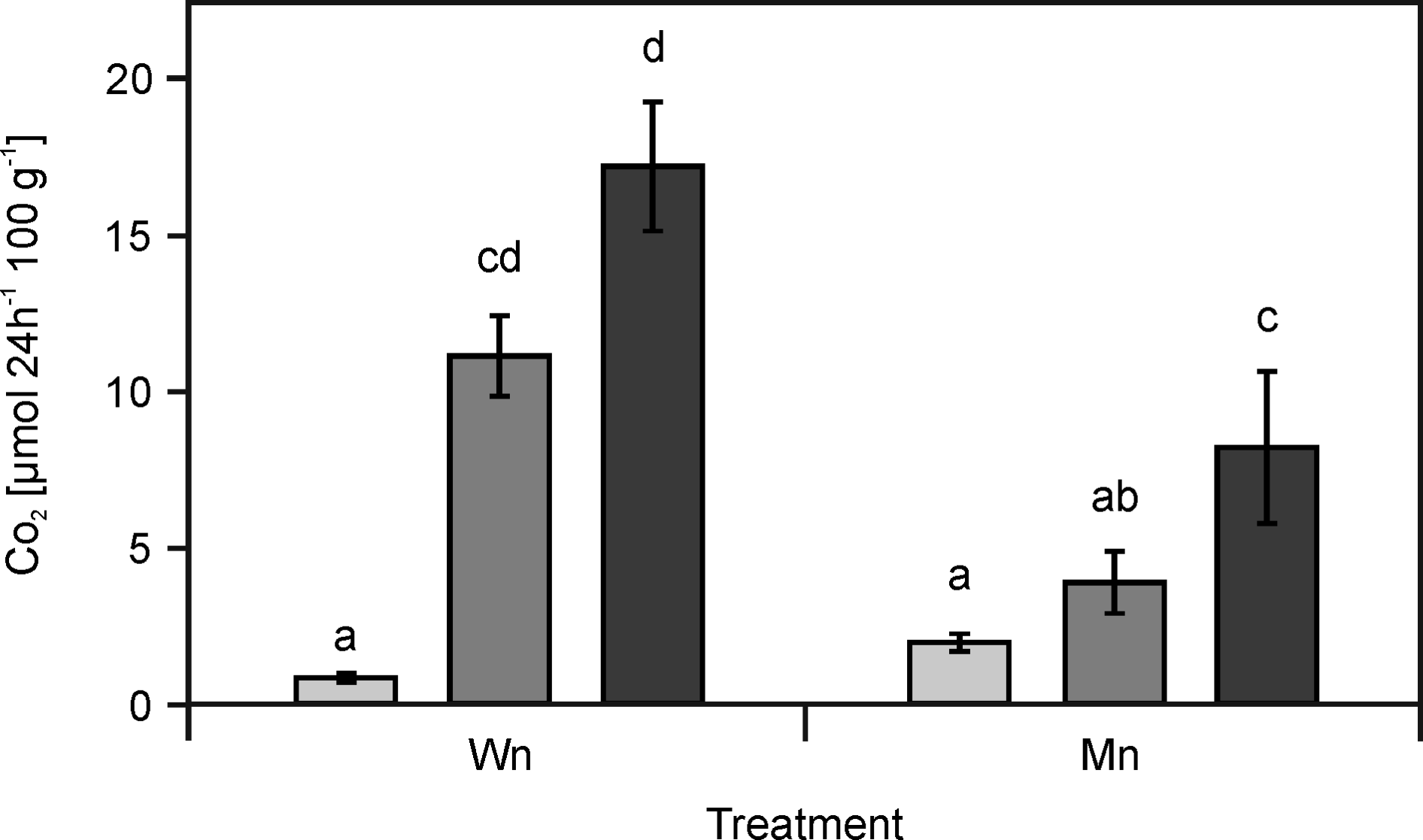
20
15
10
5
0
Co_2 [µmol $24h^{-1}$ 100 g^{-1}]
a
cd
d
a
ab
c
Wn
Mn
Treatment

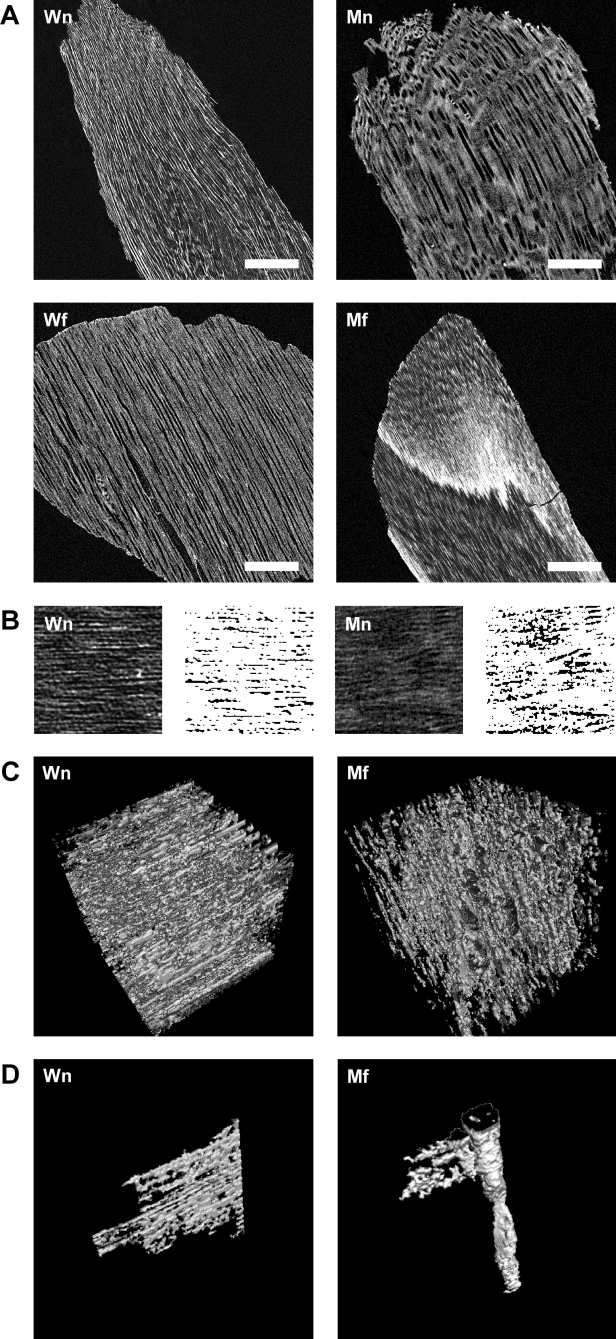
A
Wn
Mn
Wf
Mf
B
Wn
Mn
C
Wn
Mf
D
Wn
Mf

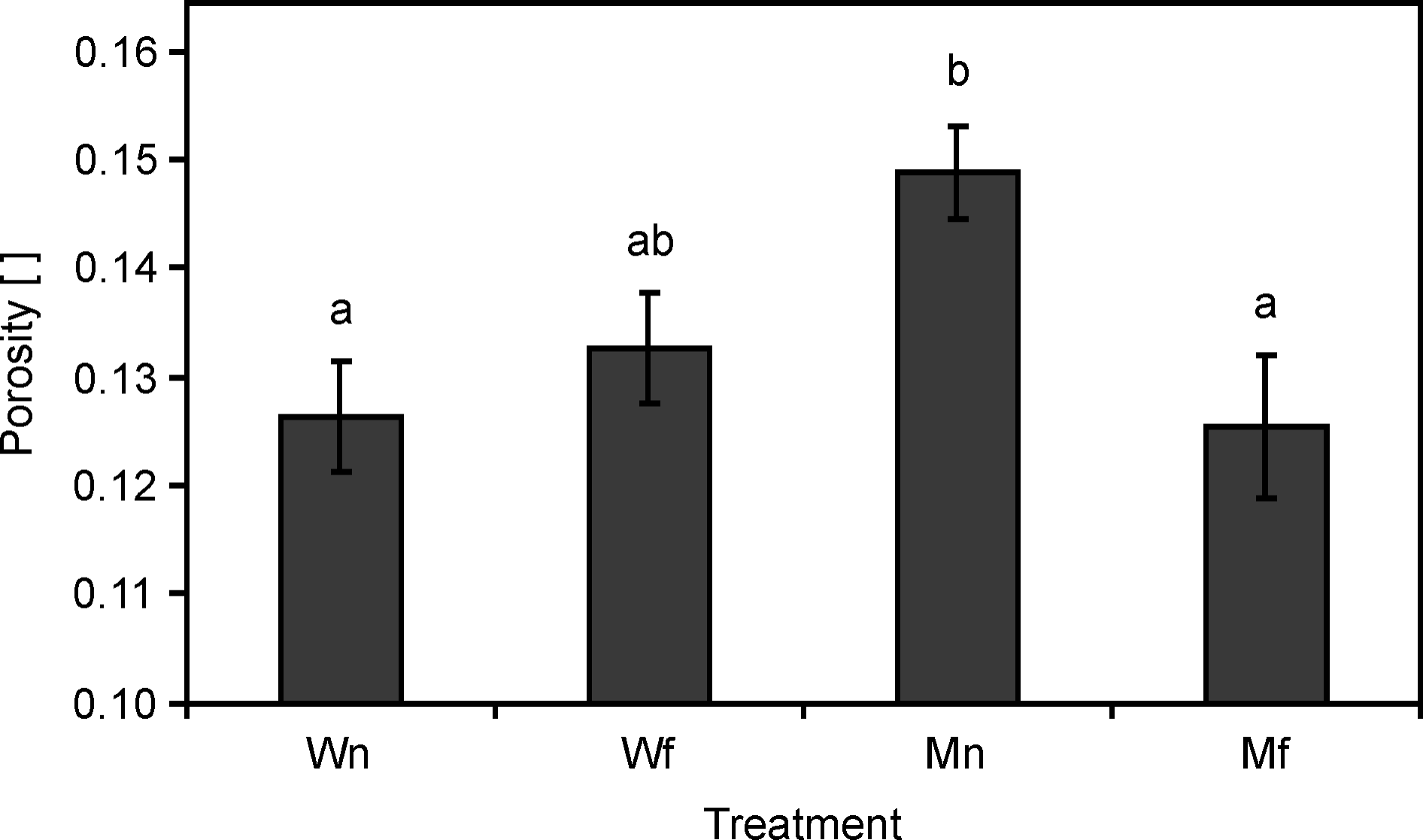
0.16
0.15
0.14
0.13
0.12
0.11
0.10
Porosity [ ]
a
ab
b
a
Wn
Wf
Mn
Mf
Treatment

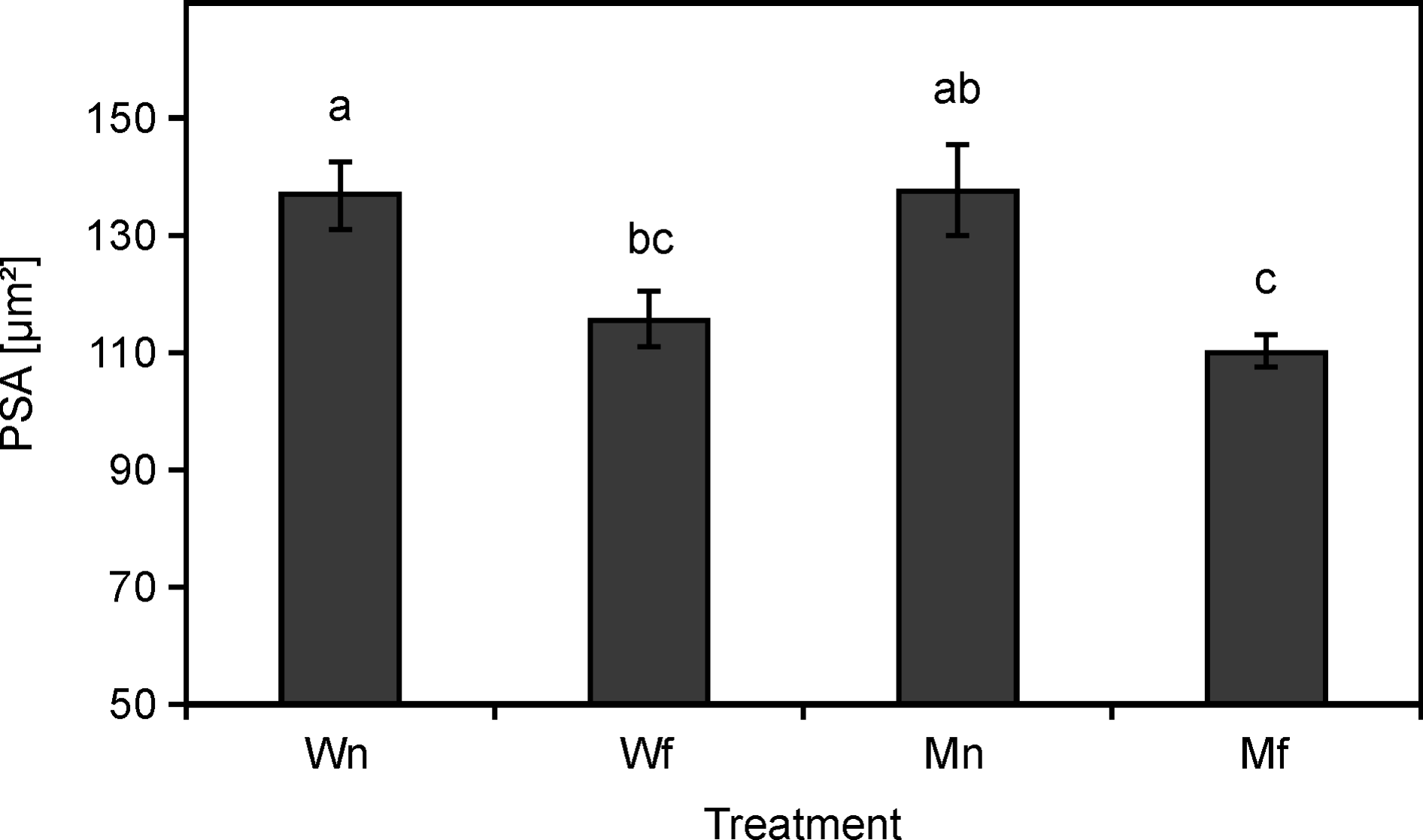
150
130
110
90
70
50
PSA [µm²]
a
bc
ab
c
Wn
Wf
Mn
Mf
Treatment

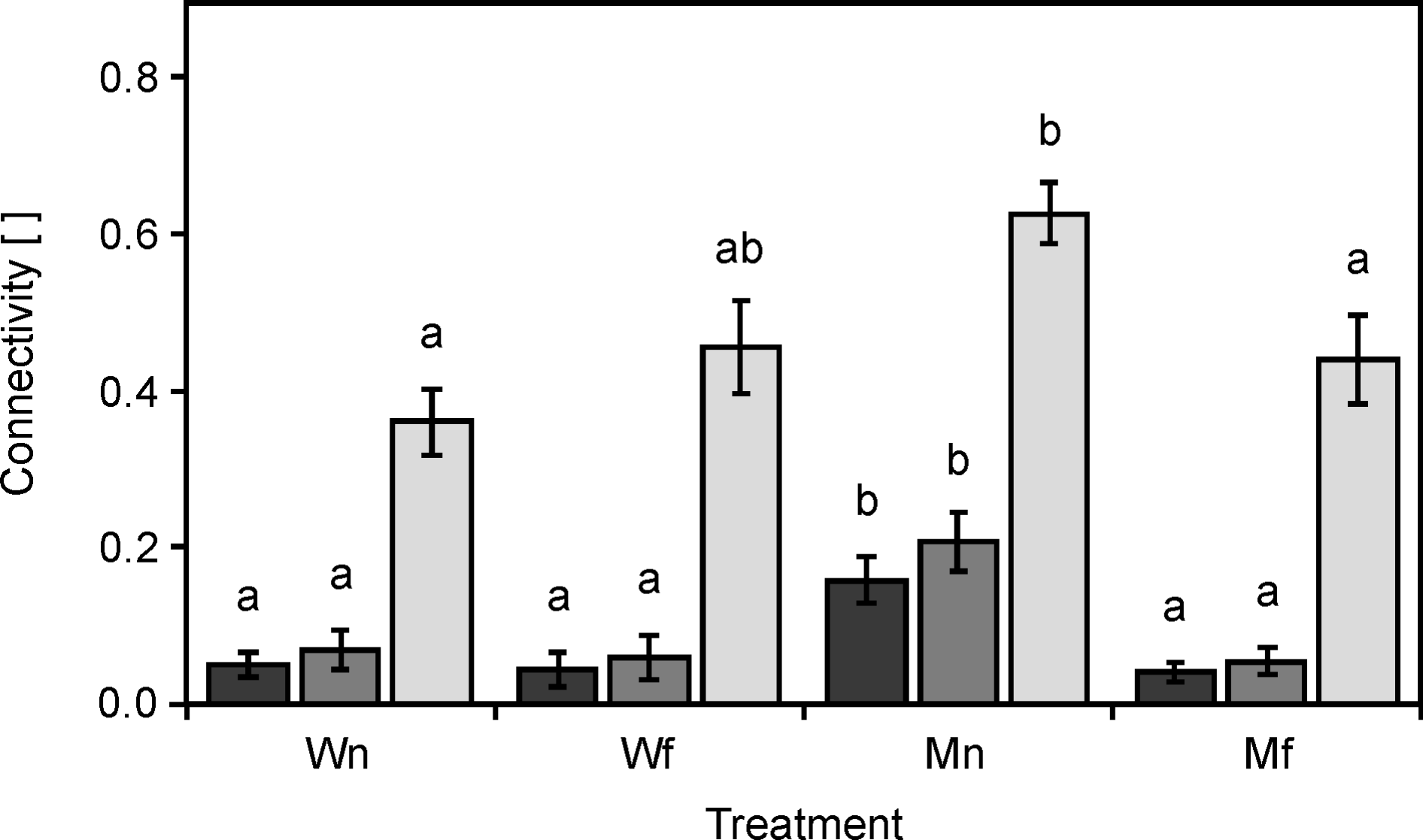
Connectivity [ ]
0.0
0.2
0.4
0.6
0.8
a
a
a
a
a
ab
b
b
b
a
a
a
Wn
Wf
Mn
Mf
Treatment

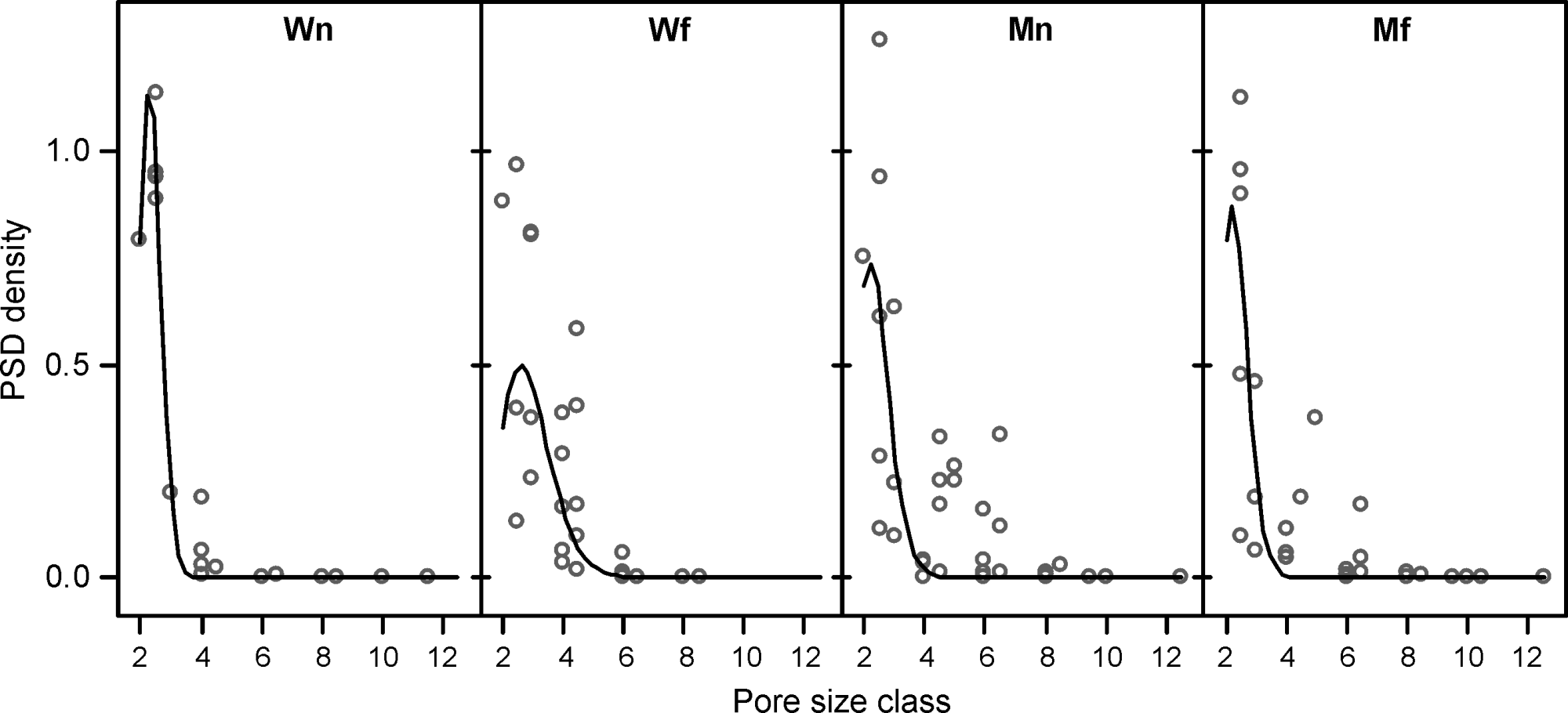
Wn
Wf
Mn
Mf
PSD density
1.0
0.5
0.0
2
4
6
8
10
12
Pore size class

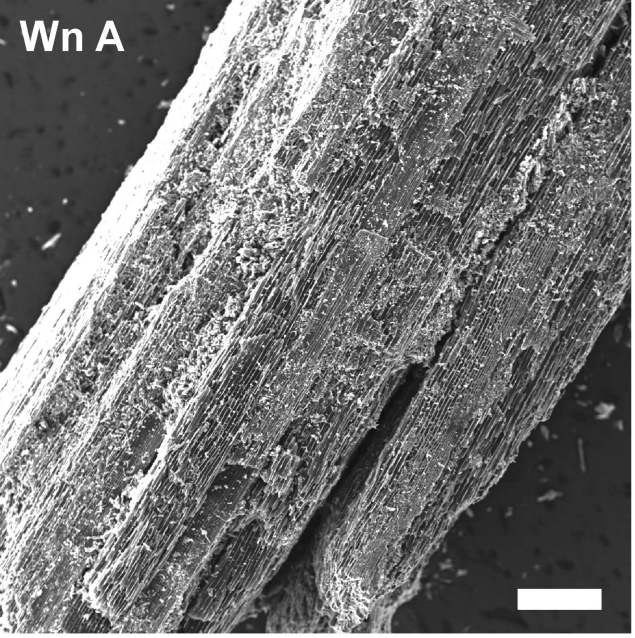
Wn A

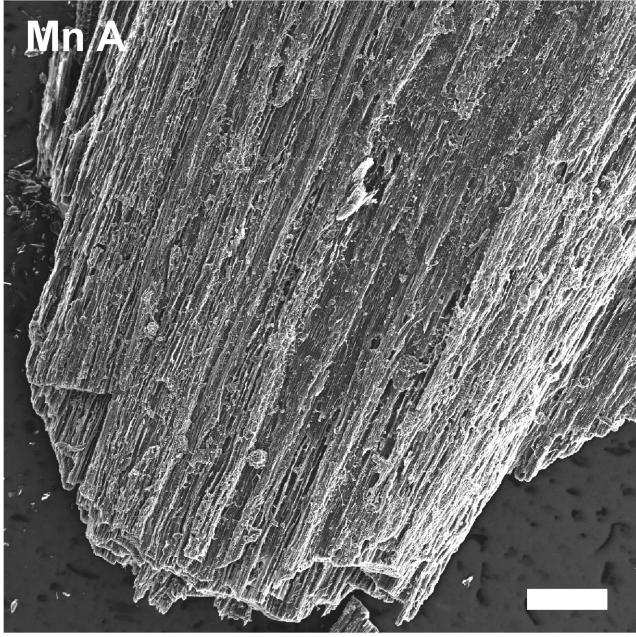
Mn A

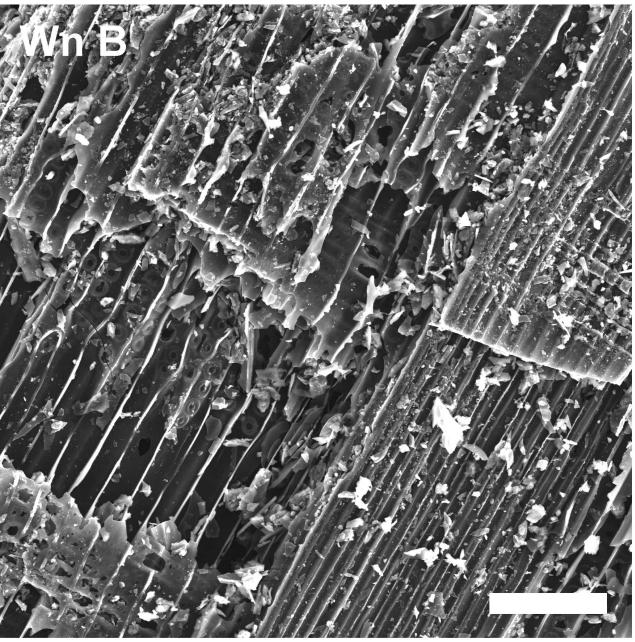
Wn B

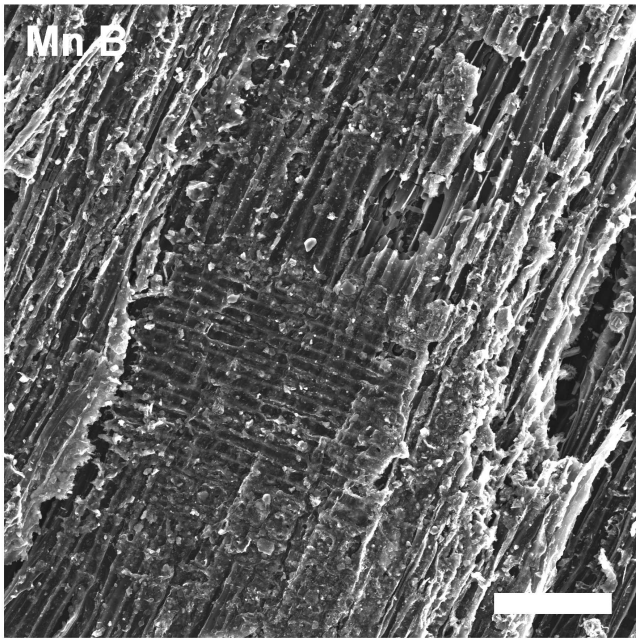
Mn B

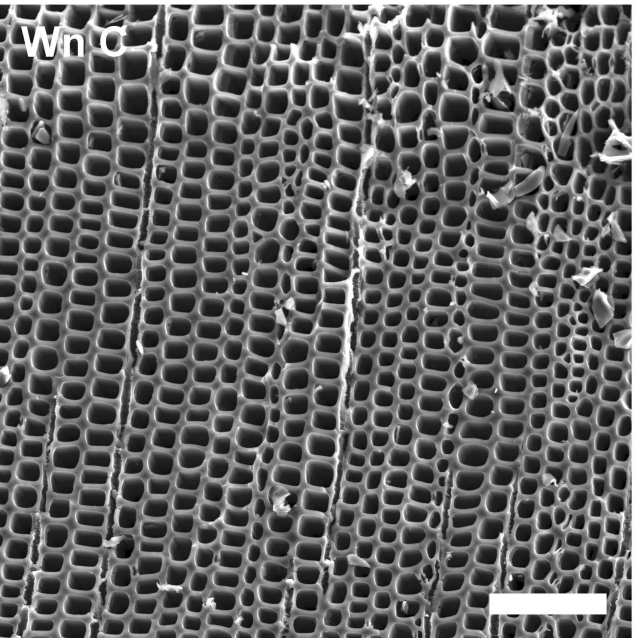
Wn C

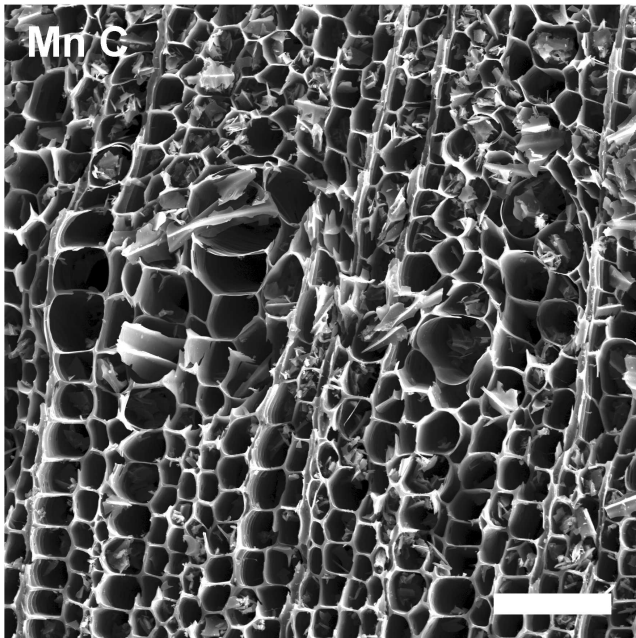
Mn C

Analysis of physical pore space characteristics of two pyrolytic biochars and potential as microhabitat

Laura S. Schnee, Stefan Knauth, Simona Hapca, Wilfred Otten, Thilo Eickhorst*

*) eickhorst@uni-bremen.de

Supplementary Material

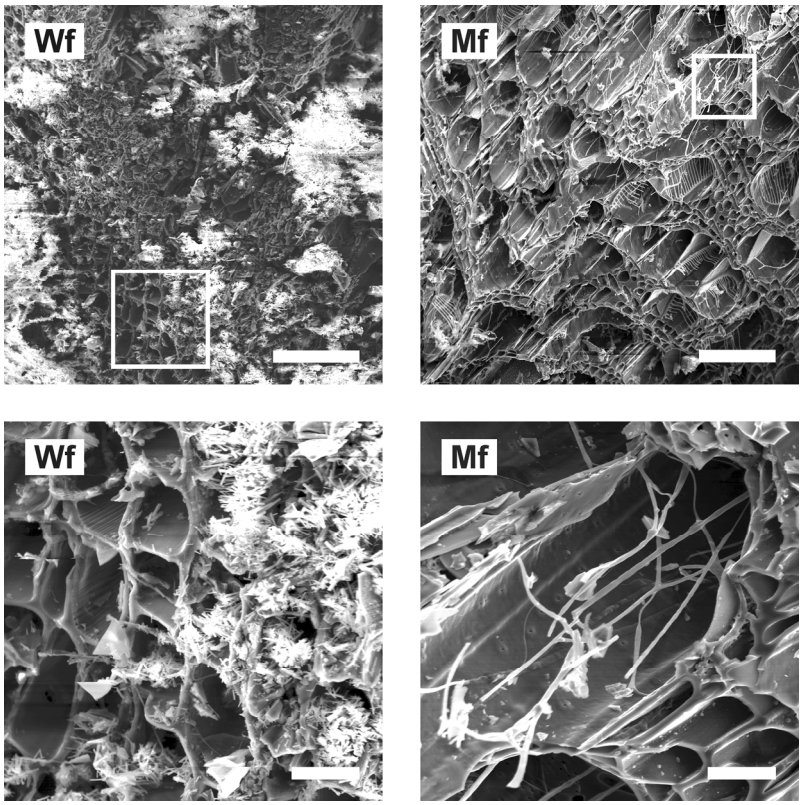

Figure S1. Fungal colonisation (*Agaricus bisporus*) on biochar particles. Mn: native Miscanthus biochar; Wn: native Wood biochar. Scale bars: Top: 100 µm; Bottom: 20 µm.

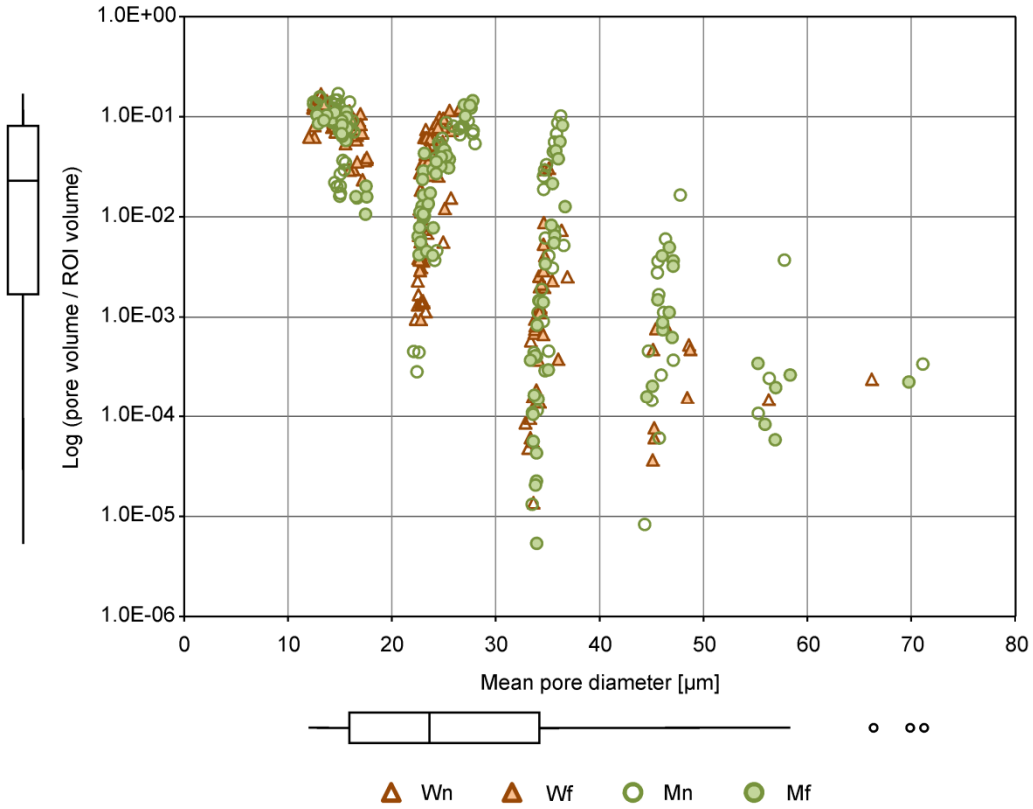

Figure S2. Scatter plot of pore size distribution (PSD) for the two biochars per treatment. Mn: Miscanthus non-colonised; Mf: Miscanthus fungi colonised; Wn: Wood non-colonised; Wf: Wood fungi colonised.

S3: DNA extraction and PCR/DGGE analysis

DNA from selected isolates was extracted by a bead-beating procedure in 2 ml reaction cups. After centrifugation and removal of liquid medium the cell pellet was resuspended in extraction buffer (100 mM Tris, 50 mM EDTA, 50 mM NaCl, 0.5 % SDS (w/v),100 µg ml-1 Proteinase K, final concentrations) and incubated at 50°C for 10 min. Sterile glass beads were added (700 mg, 1 mm diameter; 400 mg, 0.1 mm diameter) and the cups were shaken in a mixer mill (MM200, Retsch, Germany) at 25 Hz for 30 s. Proteins were removed by ammonium acetate and DNA was precipitated by the addition of one volume of isopropanol. The DNA was washed with 70 % ethanol, air dried, dissolved in TE buffer and stored at 20°C. For fungal DNA extraction the mycelium was first air dried and disrupted by pestling in extraction buffer followed by the glass bead extraction as described above.

The 16S rRNA genes were amplified using universal bacterial primers Gm5F (with gc clamp) and 907r (Muyzer et al. 1995). A touchdown program was conducted with an initial denaturation at 95°C for 60 s, followed by 13 cycles of 30 s denaturation at 95°C, annealing for 25 s at 57°C with a decrement of 0.5°C per cycle and an extension at 72°C for 13 s.

Additional 20 cycles were applied with 20 s of denaturation, 25 s of annealing and 13 s of extension. A final extension of 30 min was done for all PCRs to eliminate artefactual double DGGE bands resulting from possible heteroduplexes (Janse et al. 2004). The reactions had a volume of 50 µl containing 5 µl of DreamTaq buffer, 1.25 U DreamTaq polymerase and 20 µg of BSA (Fermentas, Germany). The final concentrations were 0.5 µmol l-1 of each primer and 50 µmol l-1 of each nucleotide.

The PCR fragments were separated by denaturing gradient gel electrophoresis (DGGE) with a 50 to 70 % denaturing gradient (100 % denaturant contained 7 mol l-1 urea and 40 % (v/v) deionized formamide) at 60°C and 60 V for 16 h using a DGGE 2001 apparatus (CBS Scientific, USA). Selected bands of different gel positions were excised, reamplified by PCR and purified for later sequencing.

The fungal strains were selected by colony morphology. The 18S rRNA genes were PCR amplified using the NS1 and EF3 primers (Hoshino & Morimoto 2008). The PCR programme was conducted with an initial denaturation at 94°C for 120 s, followed by 25 cycles of 15 s denaturation at 94°C, annealing for 30 s at 47°C and an extension at 72°C for 120 s followed by a final extension of 8 min. The content of the PCR reactions were the same as for bacteria with the exception that the final MgCl2 concentration was 3 mM.

References

Hoshino YT, Morimoto S (2008) Comparison of 18S rDNA primers for estimating fungal diversity in agricultural soils using polymerase chain reaction-denaturing gradient gel electrophoresis. Soil Science and Plant Nutrition, 54(5), 701–710.

Janse I, Bok J, Zwart G (2004) A simple remedy against artifactual double bands in denaturing gradient gel electrophoresis. Journal of Microbiological Methods 57, 279-281.

Muyzer G, Teske A. Wirsen CO, Jannasch HW (1995) Phylogenetic relationships of Thiomicrospira species and their identification in deep-sea hydrothermal vent samples by denaturing gradient gel electrophoresis of 16S rDNA fragments. Archives of Microbiology, 164, 165-172.